Langmuir

Article

pubs.acs.org/Langmuir

Potential Determining Salts in Microemulsions: Interfacial Distribution and Effect on the Phase Behavior

Christoffer Johans,*[,†] Manja A. Behrens,[‡] Karl Erik Bergquist,[‡] Ulf Olsson,[‡] and José A. Manzanares[§]

[†]Department of Chemistry, Aalto University, P.O. Box 16100, FI-00076 Aalto, Finland

[‡]Physical Chemistry, Lund University, P.O. Box 124 SE-221 00 Lund, Sweden

[§]Faculty of Physics, Department of Thermodynamics, University of Valencia, c/Dr. Moliner, 50, E-46100 Burjasot, Spain

Supporting Information

ABSTRACT: In this work we consider potential determining salts, also referred to as phase transfer agents for a future objective of electrochemistry at the oil−water interface in microemulsions. We have studied these salts, composed of a hydrophilic and a hydrophobic ion, in microemulsion stabilized by nonionic surfactants with an oligo ethylene oxide headgroup. NMR measurements show that the salts preferentially dissociate across the surfactant interface between the oil and water domains, and hence create a potential drop across the surfactant film, and back to back diffuse double layers in the oil and water phases. These observations are also supported by Poisson−Boltzmann calculations. This adsorption like event stabilizes the microemulsion. Repulsive long-range interactions between thin lamellae of surfactant and water lamellae in oil were observed using SAXS, thus confirming the presence of electrostatic forces mediated through the oil domain. We also observed that reversing the charges on the potential determining salts had opposite effects on the phase inversion temperature.

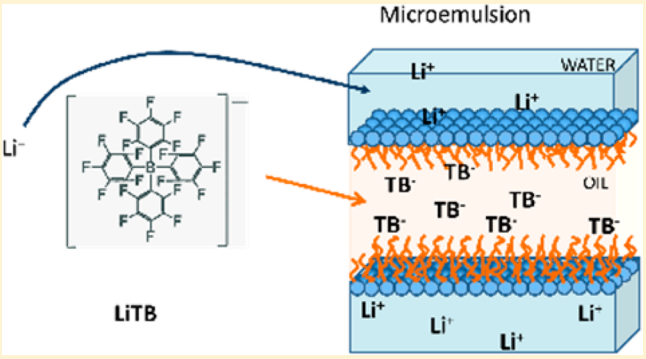

1. INTRODUCTION

Microemulsions are typically water−oil mixtures, stabilized by a surfactant.[1] They can simultaneously solubilize large amounts of hydrophilic and hydrophobic solutes; however, they also offer a very large oil−water interface. In this work we consider fundamental characteristics of microemulsions for a future objective of electrochemistry at their oil−water interface. It is relevant to explore how the morphology is affected when the interface is polarized for this purpose. In the absence of external electrodes, polarization can be induced using so-called potential determining salts that are composed of a hydrophilic and a hydrophobic ion. Such salts affect the distribution potential across the interface.[2] Markin and Volkov have shown in a theoretical study[3] that in small oil−water systems droplets are expected to be non-electroneutral. This occurs when the interface becomes large in comparison to the bulk volumes.

Previous studies on the morphology of microemulsions have shown that it can vary from discrete swollen micelles in solution to disordered bicontinuous networks as a function of either temperature or composition.[4] Typically in one phase microemulsion, oil-droplets-in-water (L_1) are observed at low temperatures, bicontinuous (L_3) or lamellar (L_α) at intermediate temperatures, and water-droplets-in-oil (L_2) at high temperatures. The phase behavior has been well explained using the flexible surface model,[6−11] in which the free energy of the system is dictated by the curvature free energy and the mixing entropy. In this model, the surfactant film has a spontaneous curvature (H_0), and any deviation from this curvature leads to an increase of the curvature free energy. This is opposed by the entropy that strives to increase disorder. The C_nE_m surfactant systems are useful model systems because H_0 can be conveniently tuned by varying the temperature.[12−14] Increasing temperature decreases solvation of the headgroup, and consequently the spontaneous curvature changes toward the water phase. Hence, the transition from the L_1 phase through the L_3 and L_α to the L_2 phase is observed. At lower temperatures the surfactant film prefers to curve toward the oil ($H_0 > 0$), while at higher temperatures, the preferred curvature is toward water. $H_0 = 0$ at the so-called phase inversion temperature, PIT, known from emulsion science. C_nE_m stabilized emulsions can invert from oil-in-water to water-in-oil upon heating from lower temperatures, and vice versa.

The effects of ordinary salts have long been known to change the phase behavior of C_nE_m microemulsions.[15,16] These act by increasing (salting in) or decreasing (salting out) the solubility of the headgroup in water depending on the salt, in agreement with the Hofmeister series.[17] Typically, the phase inversion temperature is lowered by 10 °C/M salt.[18]

Here, we show that by addition of salts composed of a hydrophilic and a hydrophobic ion (potential determining salts) to the microemulsion, the salt primarily dissociate across

Received: March 28, 2013
Published: November 25, 2013

the interface, i.e., the hydrophobic ion is on the oil side of the surfactant monolayer and the hydrophilic ion on the water side. This has a profound effect on the phase behavior by both stabilizing the microemulsion and affecting the curvature of the surfactant film. Interestingly, we observed opposite effects when structurally similar salts with reversed charges were used. Hydrophobic cations with hydrophilic anions were found to increase the phase inversion temperature, while hydrophilic cations with hydrophobic anions decreased the phase inversion temperature.

2. EXPERIMENTAL SECTION

Materials. MQ-water was used throughout. α,α,α-Trifluorotoluene (TFT, Aldrich, >99%) was filtered over activated alumina. Tergitol NP10 was used as received. Typically, this type of surfactant contains a distribution of lengths of the oligo ethoxide headgroup; see Supporting Information for a characterization. In some samples the aqueous phase contained 10 mM LiOH (P.A., Riedel-de Haën) or 10 mM NaCl (Aldrich, >99.5%). Stock solutions of lithium tetrakispentafluorophenyl borate ethyl etherate (LiTB, Boulder Scientific) and bis(triphenylphosphoranylidene)ammonium chloride (BACl, Fluka) were prepared in ethanol. The desired amount of stock solution was placed in the used glass test tube and evaporated to dryness. In the case of LiTB the ether molecules were also evaporated in the process. The microemulsions were prepared by weighing the oil, surfactant, and water into the vessels, mixing vigorously, and adjusting the temperature to achieve homogeneous clear microemulsions (Winsor IV). All fractions, Φ_i, are given on the volume scale. The salts and chemicals used are shown in Figure 1.

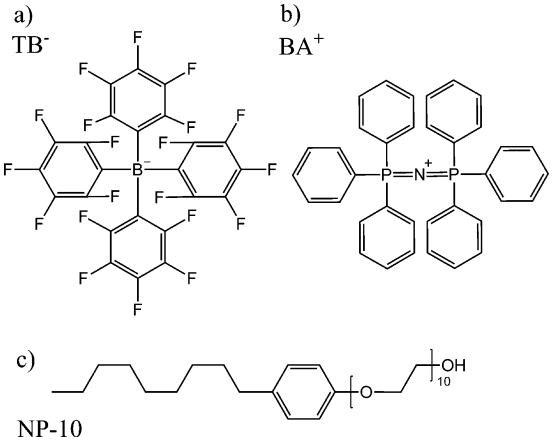

Figure 1. Structure of (a) the TB^- ion, (b) the BA^+ ion, and (c) the Tergitol NP-10 surfactant.

Methods. Samples used for the characterization of the phase diagram were flame-sealed in test tubes. The phase behavior was determined along the $\Phi_w/\Phi_o = 1$ line (corresponding to mass fraction ratio of 1/1.19), by immersing the samples in a water bath at the desired temperature. The lamellar phase was identified using cross polarizers. The temperature was changed a maximum of 1 °C, followed by an equilibration time of at least 20 min.

ζ-potentials were measured on a Malvern Zetasizer ZS instrument with a universal dip cell ζ-potential probe. The surfactant volume fraction was 0.15. The temperature was adjusted inside the one phase microemulsion body close to the emulsification failure borders, i.e., 16 °C for oil droplets in water (L_1) and 34 °C for water droplets in oil (L_2), and allowed to equilibrate for one hour in the instrument.

^{19}F and ^{7}Li NMR experiments were carried out on an Origin Avance 500 MHz instrument following standard procedure. The samples were 10 mM LiTB in water, 10 mM LiTB in TFT, and 10 mM LiTB in microemulsion with 42.5% water, 42.5% TFT, and 15% Tergitol NP10. A capillary filled with D_2O in the sample was used for signal lock. The microemulsion was lamellar at the measurement temperature of 21.3 °C.

The Small Angle X-ray Scattering (SAXS) experiments were performed on a Ganesha 300XL instrument (JJ X-ray Systems) using a 3 pinhole setup. This instrument is equipped with a Pilatus detector and the radiation is generated by a microfocus source giving a wavelength of 1.54 Å. The entire system is evacuated during measurements. The samples were kept in reusable quartz capillaries and temperature control was obtained by placing the capillaries in a thermostatted block circulating water. The samples were measured for 3600 s and so were the subsequent backgrounds. Water was used as a primary standard for absolute calibration of the scattering data. The samples were prepared by mixing surfactant, oil, and 5 or 10 mM LiTB(w) at constant $\Phi_w/\Phi_S = 1$ in TFT with $\Phi_o = 0.6$, 0.65, and 0.7. The temperature was kept constant at 30 °C (±0.1 °C) for all samples, except $\Phi_o = 0.7$, which was at 33 °C for 5 mM LiTB(w) and 36 °C for 10 mM LiTB, respectively. These temperatures were chosen to be well within the temperature range of the lamellar phase. In the fitting model, the lamellas (form factor) were assumed to be of uniform density throughout. The scattering length density difference (SLD) between the lamellae and the solvent was taken as an adjustable parameter. The coefficient of variation for the fitted SLDs was 8.5%.

RESULTS

Phase Behavior. α,α,α-Trifluorotoluene was chosen as the oil in this study, since it is suitable for electrochemical studies at oil−water interfaces, which is a future objective of this study. The Kahlweit's fish diagram in the T−X plane at constant oil to water (10 mM LiOH) ratio equal to one ($\Phi_w/\Phi_o = 1$) is shown in Figure 2. The phase behavior in the absence of LiTB shows

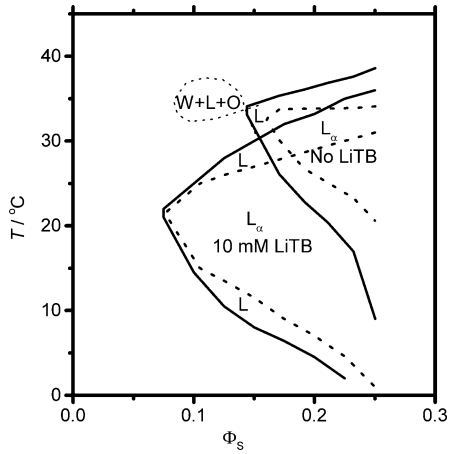

Figure 2. Kahlweit's fish diagram[19] of the system Tergitol NP10−10 mM LiOH(w)−TFT showing how the phase behavior evolves with temperature and surfactant volume fraction (Φ_S) at the constraint of equal fractions of water and oil ($\Phi_w = \Phi_o$). The upper diagram corresponds to no added LiTB and the lower to the presence of 10 mM LiTB. The dashed lines denote the boundary between the lamellar and the microemulsion phases. At fractions below 0.1 the lamellar phase boundary could not be distinguished from the emulsion failure boundaries. Notice that the three phase body (W+L+O) is shown only for clarity and has not been determined through thorough experiments.

typical behavior for microemulsions stabilized by surfactant with PEO head groups, i.e., the surfactant monolayer curves toward oil leading to oil-droplets-in-water at low temperatures and toward the water phase at high temperatures resulting in water-droplets-in-oil. The emulsion failure boundaries, where a droplet microemulsion is in equilibrium with the excess internal phase, are reached when the curvature of the droplets becomes

dx.doi.org/10.1021/la404263v | Langmuir 2013, 29, 15738−15746

too large to absorb all of the internal phase. At intermediate temperature ranges, either the bicontinuous, at lower concentrations, or the lamellar phase at higher concentrations is found. The ordered lamellar phase was identified by the birefringence apparent between crossed polarizers. The phase inversion temperature was 34 °C and a surfactant volume fraction of 0.14. We have focused on the "fish tail", i.e., the one phase microemulsion body. The three phase body with microemulsion in equilibrium with excess water and oil phases also exists in absence of LiTB. The solubility of Tergitol NP-10 in the excess trifluorotoluene was determined to equal 8% using standard gravimetric procedure. This finding agrees well with partitioning determined from SAXS, as will be shown later on in this study.

Since the Tergitol NP-10 used was not further purified, the presence of a distribution of chain lengths cannot be discarded (see Supporting Information). It is known that, contrarily to pure ones, lower grade surfactants show a distortion of the phase boundaries, especially at low surfactant concentrations (i.e., the distortion affects mostly to the three phase body, though not only).[20] These effects are often associated with a higher monomeric solubility of the surfactant in oil. The phase diagrams in Figure 2 do not compare to those distorted phase diagrams.

In the presence of 10 mM LiTB, the minimum surfactant fraction required to obtain a one phase microemulsion decreases to $\Phi_S = 0.075$. We did not observe the three phase body, which is reasonably explained by the fact that the one phase region extends almost all the way to the limit set by the solubility of the surfactant in the oil phase. We suggest that the stabilization of the one phase microemulsion with respect to the two phase regions is due to the lowering of the free energy due to partitioning of the Li^+ and TB^- ions at opposite sides of the interface, which is driven by the difference in preferential solvation of the ions. In this respect the potential determining salt has a strong surfactant like character, causing it to adsorb at the interface. Salts have previously been observed to stabilize microemulsions; however, the effect is notable only at much higher concentrations than applied here.[18] The lamellar phase boundaries at lower Φ_s are extended all the way to the emulsion failure boundaries, which suggests that the interface has become stiffer, .i.e., the undulations of the surfactant monolayer are smaller. The phase inversion temperature (PIT) was lowered from 34 to 22 °C. When compared to conventional salts like NaCl, the lowering of the PIT is 2−3 orders of magnitude larger than what has been commonly found in C_mE_n stabilized microemulsions.[18] The change is on the same order of magnitude as the addition of common ionic surfactants to C_mE_n stabilized microemulsions,[21] where the ionic surfactant induces an electric double layer that in turn imposes a curvature strain on the surfactant monolayer. The strong interaction we have observed here indicates that the salt interacts strongly with the interfacial surfactant film; however, in this case electrical double layers occur on both sides of the surfactant monolayer. The addition of LiTB also shifts the phase inversion temperature toward lower temperatures, while ionic surfactants raise the phase inversion temperature. As will be shown later, the sign of the change of the phase inversion temperature depends on the salt, e.g., the addition of BACl to the microemulsion results in an increase of the phase inversion temperature.

Poisson−Boltzmann Model of Ion Distributions. Potential determining salts have been extensively studied at bulk oil/water interfaces. The main difference between the studies at bulk interfaces and the microemulsion studied here is that in the latter one cannot assume that the oil or the water remains electroneutral due to the small length scales.[3,22] Assume that we have an aqueous solution with a molar concentration C of a 1:1 electrolyte and that, when this aqueous phase is in contact with an oil phase, the distribution equilibrium is such that the cations are basically only present in the aqueous phase and the anions are only present in the organic phase (this assumption is justified later on). The two phases have a lamellar structure that is described here as alternating planar slabs, or aqueous and oil phases separated by surfactant monolayers. Using the cell model,[23,24] half aqueous slab, one surfactant monolayer and half organic slab are considered in the following description of the electrical interfacial structure. d_w, d_o, and d_s denote the half-thickness of the aqueous and oil slab, and the surfactant monolayer. The half aqueous slab occupies the region $0 \le x \le d_w$, the surfactant monolayer the region $d_w \le x \le d_w + d_s$, and the half organic slab $d_w + d_s \le x \le d_w + d_s + d_o$. Their respective relative electrical permittivities are ε_w, ε_s, and ε_o. Assuming that the ions cannot be present in the surfactant monolayer, the Poisson−Boltzmann equation of this system is

$$\varepsilon_0 \frac{d^2\phi}{dx^2} = \begin{cases} -\dfrac{Fc_{w0}e^{-f(\phi-\Delta_o^w\phi)}}{\varepsilon_w}, & 0 \le x \le d_w \\ 0, & d_w \le x \le d_w + d_s \\ \dfrac{Fc_{o0}e^{f\phi}}{\varepsilon_o}, & d_w + d_s \le x \le d_w + d_s + d_o \end{cases} \quad (1)$$

where ϕ is the electric potential, F is Faraday's constant, ε_o is the vacuum electrical permittivity, c_{w0} is the cation concentration at $x = 0$, where the electric potential is $\phi(0) = \Delta_o^w\phi$, and c_{o0} is the anion concentration at $x = d_w + d_s + d_o$, where the electric potential is taken as zero. The electric field is zero at $x = 0$ (mid water layer) and $x = d_w + d_s + d_o$ (mid oil layer) due to symmetry requirements. The values of c_{w0} and c_{o0} are determined from the conditions of conservation of the amounts of ions

$$Cd_w = \int_0^{d_w} c_{w0}\, e^{-f(\phi-\Delta_o^w\phi)}\, dx = \int_{d_s+d_o}^{d_w+d_s+d_o} c_{o0}\, e^{f\phi}\, dx \quad (2)$$

For the sake of convenience, we also introduce $\sigma \equiv FCd_w$ as the charge density separated across the surfactant monolayer. By Gauss' law, this quantity is related to the electric field at the external boundaries of the surfactant monolayer as well as in its interior

$$\varepsilon_w\left(\frac{d\phi}{dx}\right)_{x=d_w-} = \varepsilon_o\left(\frac{d\phi}{dx}\right)_{x=d_w+d_s+} = \varepsilon_s\left(\frac{d\phi}{dx}\right)_{\text{surfactant}} = -\frac{\sigma}{\varepsilon_0} \quad (3)$$

Introducing the Debye parameters

$$\kappa_w^2 \equiv \frac{2F^2c_{w0}}{\varepsilon_0\varepsilon_w RT} \qquad \kappa_o^2 \equiv \frac{2F^2c_{o0}}{\varepsilon_0\varepsilon_o RT} \quad (4)$$

the dimensionless position variables $\xi_w \equiv \kappa_w x$, $\xi_o \equiv \kappa_o(d_w + d_s + d_o - x)$, and the dimensionless electric potentials $\varphi_w \equiv F(\Delta_o^w\phi$

dx.doi.org/10.1021/la404263v | Langmuir 2013, 29, 15738−15746

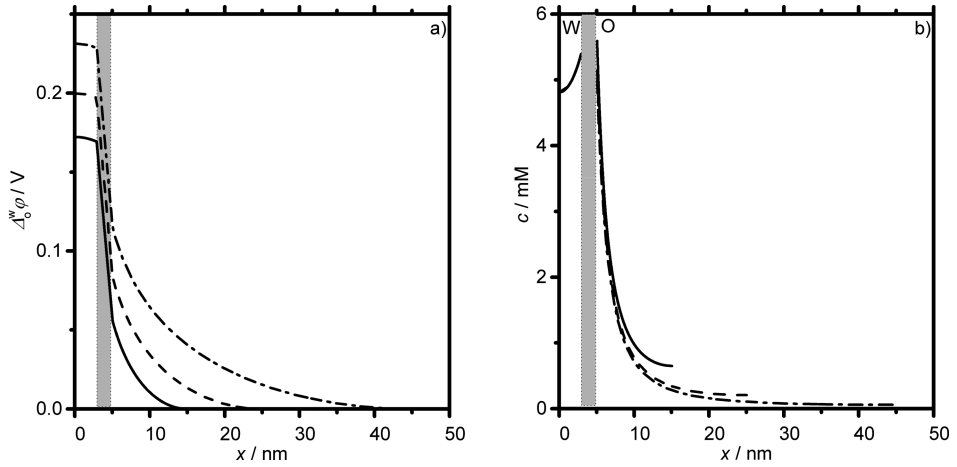

Figure 3. (a) Potential profiles for the 5 mM LiTB (calculated with respect to only the water phase). (b) Concentration profiles for Li^+ (water) and TB^- (oil) in a microemulsion. The half-thickness of the water domain was 2.93 nm, oil domain: (solid) 10, (dash) 20, and (dash-dot) 40 nm; and the thickness of the surfactant layer: 2.14 nm.

$-\phi)/RT$ and $\varphi_o \equiv F\phi/RT$, the Poisson−Boltzmann equation in the aqueous and organic phases reduces to

$$d^2\varphi/d\xi^2 = e^{\varphi}/2 \qquad 0 \le \xi \le \xi_d \tag{5}$$

with boundary conditions $\varphi(0) = 0$, $(d\varphi/d\xi)_{\xi=0} = 0$, and its solution is

$$\varphi(\xi) = \ln[1 + \tan^2(\xi/2)] = -2\ln[\cos(\xi/2)] \tag{6}$$

Equation 6 implies that the relation between the values of φ and its derivative at ξ_d is

$$(d\varphi/d\xi)_{\xi_d} = \sqrt{e^{\varphi(\xi_d)} - 1} = \tan(\xi_d/2) \tag{7}$$

Combining eqs 2, 3, and 7 we can derive the algebraic equations that allow for the determination of c_{w0} and c_{o0}, as well as the total potential difference from the center of the organic slab to that of the aqueous slab

$$C = c_{w0}\frac{\tan\left(\sqrt{\frac{2F^2c_{w0}}{\varepsilon_0\varepsilon_w RT}}\frac{d_w}{2}\right)}{\sqrt{\frac{2F^2c_{w0}}{\varepsilon_0\varepsilon_w RT}}\frac{d_w}{2}} = \frac{d_o}{d_w}c_{o0}\frac{\tan\left(\sqrt{\frac{2F^2c_{o0}}{\varepsilon_0\varepsilon_o RT}}\frac{d_o}{2}\right)}{\sqrt{\frac{2F^2c_{o0}}{\varepsilon_0\varepsilon_o RT}}\frac{d_o}{2}} \tag{8}$$

$$\Delta_o^w\phi = \frac{\sigma d_s}{\varepsilon_0\varepsilon_s} - 2\frac{RT}{F}\ln\left[\cos\left(\sqrt{\frac{2F^2c_{w0}}{\varepsilon_0\varepsilon_w RT}}\frac{d_w}{2}\right)\cos\left(\sqrt{\frac{2F^2c_{o0}}{\varepsilon_0\varepsilon_o RT}}\frac{d_o}{2}\right)\right] \ge 0 \tag{9}$$

These expressions can be simplified using series expansions when the arguments of the trigonometric functions are much smaller than 1, which only occurs for sufficiently small electrolyte concentrations.

Consider, for instance, the case $\varepsilon_w = 78$, $\varepsilon_s = 3$, $\varepsilon_o = 9.3$, $d_w = 2.93$ nm, $d_s = 2.14$ nm, $d_o = 10$ nm, and $C = 5$ mM at $T = 300$ K. Later on, the corresponding experimental system is studied by SAXS. This corresponds to a surface charge density of $\sigma = 1.413 \times 10^{-21}$ C/nm^2 separated across the surfactant monolayer (positive on the aqueous side and negative on the organic side); this is a small value, equivalent to one elementary charge per 113 nm^2, but it should be noted that 5 mM implies that the spherical volume per ion has a radius of 4.30 nm, which is larger than the half-thickness of the aqueous slab. The potential drop across the surfactant monolayer is then $\sigma d_s/\varepsilon_0\varepsilon_s = 114$ mV. From eqs 8 we obtain that $c_{w0} = 4.812$ mM and $c_{o0} = 0.655$ mM, so that the potential drops in the aqueous and organic layers are 2.9 mV and 55 mV, respectively, and the total potential drop is 172 mV; a similar calculation for $C = 10$ mM yields 317 mV. For $d_o = 10$ nm and $C = 5$ mM, the concentrations of the cation and anion at the external boundaries of the surfactant monolayer are $c_{w0}\, e^{2.9/25.8} = 5.38$ mM and $c_{o0}\, e^{55/25.8} = 5.52$ mM, respectively. Figure 3 shows the electric profile for the case discussed, as well as for the cases $d_o = 20$ and $d_o = 40$ nm and $C = 5$ mM.

The concentration of the cation at the center of the organic slab is $c_{w0}\, e^{F(\Delta_o^w\phi - \Delta_o^w\phi_+^o)/RT}$, where $\Delta_o^w\phi_+^o = \Delta_w^oG_{tr,+}^o/F$ is the standard transfer potential and $\Delta_w^oG_{tr,+}^o$ is the Gibbs free energy of transfer of the cation from the aqueous to the organic phase. In the case of Li^+ ion and TFT as organic phase, their values are $\Delta_w^oG_{tr,+}^o = 73$ kJ/mol[25−27] and $\Delta_o^w\phi_+^o = 756.6$ mV, which implies for $d_o = 10$ nm and $C = 5$ mM that $c_{w0}\, e^{F(\Delta_o^w\phi - \Delta_o^w\phi_+^o)/RT} = 0.73$ pM. Similarly, the concentration of the anion at the center of the aqueous slab is $c_{o0}\, e^{F(\Delta_o^w\phi - \Delta_o^w\phi_-^o)/RT}$. In the case of the TB^- ion and TFT as organic phase, the Gibbs free energy of transfer of the anion from the aqueous to the organic phase is $\Delta_w^oG_{tr,-}^o = -59.5$ kJ/mol[25−27] and the standard transfer potential is $\Delta_o^w\phi_-^o = -\Delta_w^oG_{tr,-}^o/F = 616.7$ mV, which implies for $d_o = 10$ nm and $C = 5$ mM that $c_{o0}\, e^{F(\Delta_o^w\phi - \Delta_o^w\phi_-^o)/RT} = 22.3$pM. These low values of the ion concentrations in the phases where they are not preferentially solvated confirms the approximation of complete separation of the ions in the two phases made when solving the Poisson−Boltzmann equation.

The main difference between the ion distribution at the bulk oil/water interface and in oil/water microemulsions is that the potential drop between the phases is fixed in the former and variable (i.e., concentration dependent) in the latter. Note also that the fact that the aqueous and organic phases are not electroneutral, that is, $c_{w0}\, e^{F(\Delta_o^w\phi - \Delta_o^w\phi_+^o)/RT} \le c_{o0}$ and $c_{o0}\, e^{F(\Delta_o^w\phi - \Delta_o^w\phi_-^o)/RT} \le c_{w0}$ implies that the total potential drop in the system is smaller than in the case of electroneutral bulk phases,

dx.doi.org/10.1021/la404263v | Langmuir 2013, 29, 15738−15746

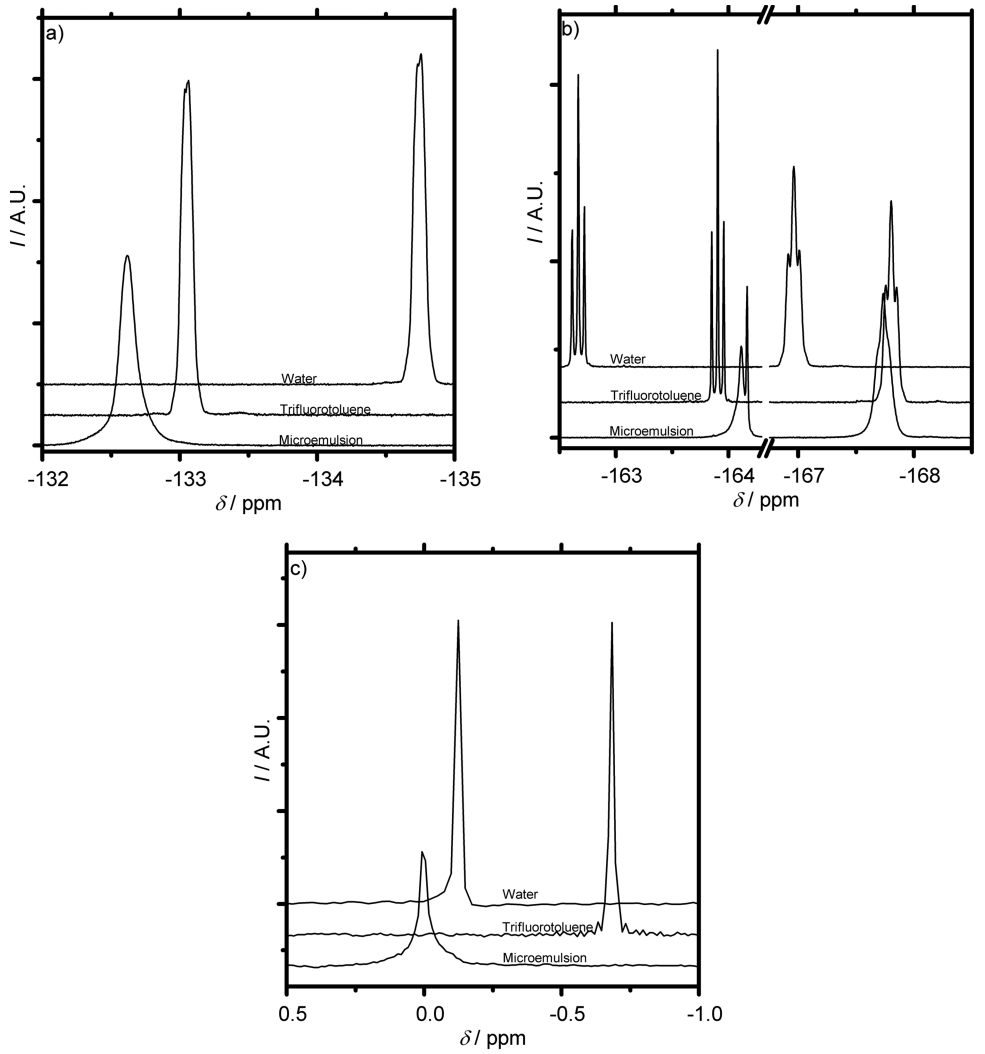

Figure 4. (a,b) ^{19}F NMR and (c) ^{7}Li NMR. Top: LiTB in water, middle TFT, and bottom microemulsion ($\Phi_w = \Phi_o = 0.425$ and $\Phi_s = 0.15$). The peaks corresponding to *o*-F are shown in (a) and *p*-F (at ≈ -163 ppm) and *m*-F (at ≈ -167 ppm) in (b).When the peak positions in the microemulsion are compared to those in water and TFT, it is seen that in the microemulsion Li^+ is in an aqueous environment and TB^- in an oil environment.

$\Delta_o^w\phi \leq (\Delta_o^w\phi_+^o + \Delta_o^w\phi_-^o)/2 = 687$ mV. In the case of electroneutral bulk phases, the electrostatic energy of the system is smaller in spite of the larger magnitude of the potential difference, because the diffuse layer is confined to the close vicinity of the surfactant monolayer, and does not extend throughout the system as in the previous figures. However, in that case the solvation contribution to the free energy is larger because hydrophilic cations are forced to be in the organic phase and hydrophobic anions in the aqueous phase due to the bulk electroneutrality constraints. The complete separation of the ions turns out to be the minimum free energy configuration for the parameter values here considered (i.e., nanometric lamellae).

ζ-Potential Measurements. To compare with experiments, we measured the ζ-potential of the droplets in a microemulsion of $\Phi_w = \Phi_o = 0.425$ and $\Phi_s = 0.15$ close to the emulsion failure boundaries, where one can reasonably assume spherical droplets of low polydispersity.[4] In the absence of LiTB, the observed potentials were distributed in the range of a few mVs for both oil droplets in water and water droplets in oil. When 10 mM LiTB was added, the ζ-potential was −1 mV on the aqueous side (oil-droplets-in-water, 16 °C) and 56 mV on the oil side (water-droplets-in-oil 34 °C), as calculated using the Hückel approximation. The experimentally accessible ζ-potential is not directly comparable to surface potentials at the surfactant monolayer, since the former is defined at the slipping plane, which is usually located a few solvent layers outside the surface. Furthermore, the geometry of the system differs, since the experimentally measured values are for droplets, while the calculated values are for lamella. Nevertheless, these differences are expected to be relatively small. When the lamellar cell model is used for $\Phi_w = \Phi_o = 0.425$ and $\Phi_s = 0.15$, the surface potential (with respect to slab center) on the aqueous side (16 °C) is −18.6 mV and the potential at an estimated slipping plane located 1 nm from surface (with respect to slab center) on the aqueous side (at 16 °C) is −11.1 mV. Similarly, for the oil side (at 34 °C), the surface potential (with respect to slab center) is +99.4 mV and the potential at a hypothetical slipping plane 1 nm from surface (with respect to slab center) on the oil side (34 °C) = +50.2 mV. Thus, we can conclude that the ζ-potentials obtained from the experiments qualitatively agree with the theoretical predictions.

^{7}Li and ^{19}F-NMR of LiTB. ^{7}Li and ^{19}F NMR spectra of 10 mM LiTB in TFT, water, and microemulsion ($\Phi_w = \Phi_o = 0.425$

dx.doi.org/10.1021/la404263v | *Langmuir* 2013, 29, 15738−15746

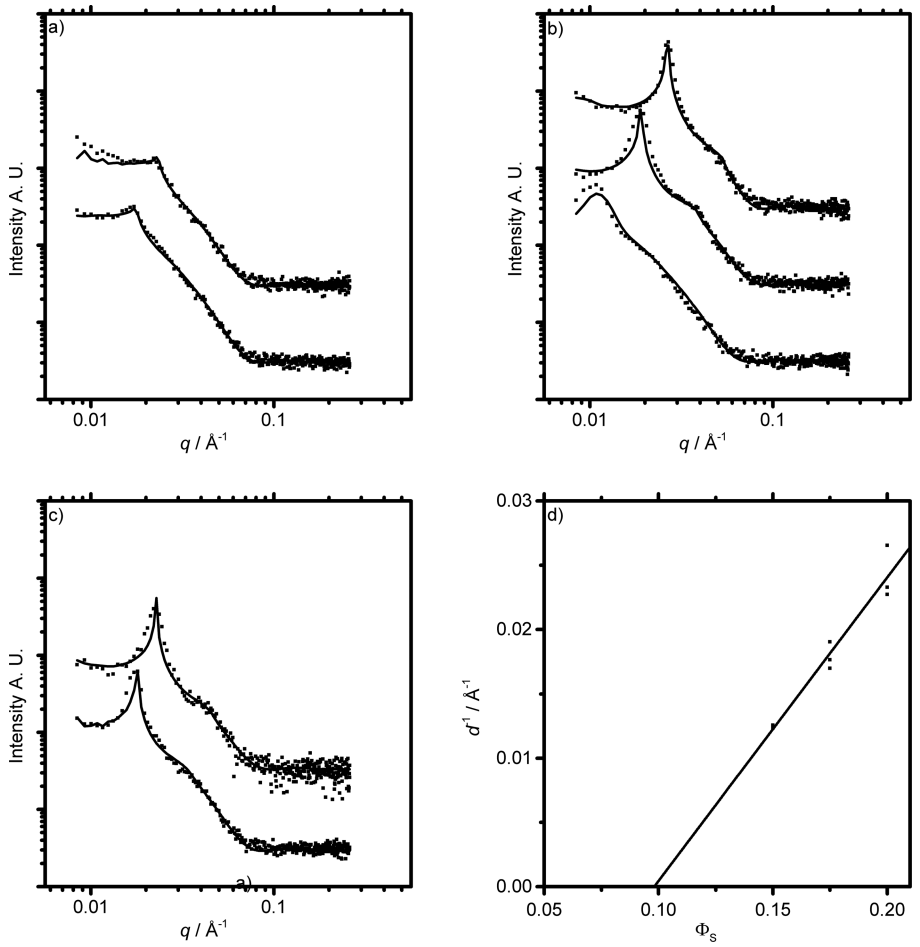

Figure 5. SAXS diffractograms and model fits for 1:1 water surfactant lamella for (a) no added LiTB and (b) 5 mM and (c) 10 mM LiTB with respect to the surfactant volume fraction. The intensity of the diffractograms have been offset for clarity: from top to bottom, Φ_o 0.6, 0.65, and 0.7, respectively. (d) Lamellar spacing d^{-1} vs surfactant fraction in the microemulsion. The intercept with the concentration axis gives a solubility of 9.7% of surfactant in the oil.

and $\Phi_s = 0.15$) are shown in Figure 4. The fluorine peak of the trifluorotoluene solvent was found at −63.76 ppm for all samples (data not shown). The assignment of the fluorine peaks of the TB^- ion in all three samples matches that expected from the literature.[28] Duplet splitting of the *o*-F peak in pure water and TFT can be seen in the vicinity of −134 ppm with a coupling constant of $\Delta\delta = 9.5$ Hz and triplet splitting of the *m*-F and *p*-F peaks at approximately 168 ppm with $\Delta\delta = 20.4$ Hz. In the microemulsion, the fluorine peaks are broader. The duplet character of the *o*-F peak cannot be resolved. Vague shoulders indicating triplet splitting can be observed at the *m*-F peak. The *p*-F is seen as a broader peak followed by a sharp peak. The area of the broad peak is twice the area of the narrow peak. Broadening of the peaks and asymmetric line shapes is well-known to occur in anisotropic media[29] and may indicate that rotational diffusion of the TB^- ion in the lamellar microemulsion phase is partially hindered. When the ^{19}F-NMR spectrum of LiTB in the microemulsion is compared with LiTB in water and TFT, it is seen that the shifts for the fluorine atoms nearly match those of LiTB in TFT. Thus, we conclude that the TB^- ion must reside in the oil phase.

The ^{7}Li peaks are observed at −0.12, −0.70, and 0.00 ppm, for LiTB in water, trifluorotolune, and the microemulsion; see Figure 4c. The similarity of the shifts in water and microemulsion indicates that Li^+ is in an aqueous environment in the microemulsion. The reason the shift is more positive in the microemulsion is not fully clear, but we suggest that extensive ion pairing between Li^+ and TB^- takes place in the water. Consequently, due to the hydrophobic TB^- ion, Li^+ experiences a less polar environment than if it was fully dissociated. On the contrary, in the microemulsion Li^+ and TB^- are on opposite sides of the interface, and ion pairing is insignificant. This hypothesis is corroborated by the shift defined for 1 M LiCl(w) at 0.00 ppm (not shown), which matches the Li^+ in the microemulsion. LiCl fully dissociates in water. Our conclusion from the NMR measurements is that LiTB dissociates across the interface, with the majority of the Li^+ in the aqueous phase and TB^- in the oil phase. This finding agrees with that predicted by the Gibbs free energy of transfer.

SAXS. The dissociation of the salt across the surfactant monolayer should result in electrostatic repulsion between the surfactant films of adjacent lamellae. While such interactions are well-known and characterized in the water phase, electrostatic repulsions mediated through the oil phase in microemulsions has not been considered to the same extent. We have chosen to study interactions in the lamellar phase using SAXS. In this case, we assume that the lamellae are composed of a layer of water between two surfactant monolayers, and adjust the distance between the lamellas by diluting with oil. The surfactant to water volume fraction ratio was constant and

dx.doi.org/10.1021/la404263v | *Langmuir* 2013, 29, 15738−15746

equal to one. Two LiTB concentrations in water of 5 mM and 10 mM were studied. Since charging of the surfactant monolayer is an interfacial process, it is of interest to consider the [LiTB]/[S] ratio as well, at least in a concentration range where the salt dissociates completely across the interface. Accounting for the finite solubility of the surfactant in the oil phase and assuming that all LiTB dissociates across the surfactant monolayer, these concentrations correspond to [LiTB/S] = 1/243−1/203 and 1/121−1/101 or, equivalently, 0.15−0.18 and 0.29−0.352 μC/cm^2, depending on the total oil concentration in the sample. The SAXS patterns are shown in Figure 5. The solid lines are best fits for Nallet et al.'s model for scattering from lyotropic lamellar phases.[30] This model takes into account the finite thickness of the lamellae and their spacing accounting for the interactions through the smectic bending elasticity, K, and the compression modulus $\bar{B}$. In the model, these appear in the form of Caillé's constant:[31]

$$\eta = \frac{q_o^2 kT}{8\pi\sqrt{K\bar{B}}}$$

q_0 is the position of the first order Bragg peak. Electrostatic interactions are reflected in both K and $\bar{B}$, and hence we cannot separate them in this analysis.

In the absence of LiTB (Figure 5a), a broad first order peak can be observed and a shoulder distinguished at double q values corresponding to the second order peak, as expected for a lamellar phase. These correspond to a lamellar spacing of 27 nm. When the oil fraction Φ_{oil} is increased from 0.6 to 0.65, the peak shifts to lower q values, corresponding to an increase of the spacing to 36 nm. The lamellar thickness was 7−7.5 nm in all samples. The spacing and thickness agree well with that expected from simple geometric arguments considering the surfactant length and volumetric ratios. The Caillé parameter was 1−1.2 for these samples, reflecting very weak interactions and/or flexible monolayers. It should be noticed that the Caillé parameter is on the limits of the applicability of the model.

In the presence of 5 mM LiTB (Figure 5b), with respect to the surfactant, the first order peak becomes much more defined, and the Caillé parameter decreases to the 0.4−0.5 range for Φ_o = 0.6 and 0.65. The corresponding spacing was 25 and 33 nm, respectively. The decrease in the Caillé parameter reflects the decrease in compressibility and/or increased stiffness of the surfactant monolayers due to electrostatic interactions.[23,32] The repulsive electrostatic force leads to smaller fluctuations of the surfactant monolayers. At Φ_o = 0.7, the distance between the spacing has increased to 51 nm and the Caillé parameter increased to 0.85. However, at this oil fraction the fit was rather insensitive to variations in the Caillé parameter. Increasing the LiTB concentration further to 10 mM (Figure 5c) does not lead to drastic changes in the fitted parameters. The Caillé parameter remained approximately equal to 0.5, in agreement with theoretical predictions that electrostatic repulsion between two surfaces is independent of surface charge[33] for highly charged surfaces.

The solubility of the surfactant in the oil phase can also be obtained from the scattering data,[34] by following the variation of the first order Bragg peak with Φ_s, i.e., spacing, d, of the lamellae; see Figure 5d. This analysis gives a solubility of 9.7%, which is in fair agreement with the gravimetrically obtained value of 8%.

Influence of the Potential Determining Salt on PIT. The temperature dependence of the one phase (microemulsion and lamellar) body is shown in Figure 6 as a function of added salts at constant composition of $\Phi_w = \Phi_o = 0.425$ and Φ_s = 0.15. LiTB is shown on the left side and BACl on the right side. The dotted line in the middle corresponds to no added salt. It is observed that the one phase body widens, i.e., the temperature range increases, with increasing concentration of the potential determining salt for both salts. Yet, the most interesting observation is that BACl moves the one phase body toward higher temperatures with increasing salt concentration, while LiTB moves the one phase body to lower temperatures. We have also observed a similar behavior in other systems (data not shown). Salts with hydrophobic anions and hydrophilic cations (Na^+ tetraphenylarsonium borate) lower the temperature of the one phase body, while hydrophobic cations and hydrophilic anions (tetraphenylarsonium chloride, tetrahexyl ammonium chloride) increase the temperature of the one phase body.

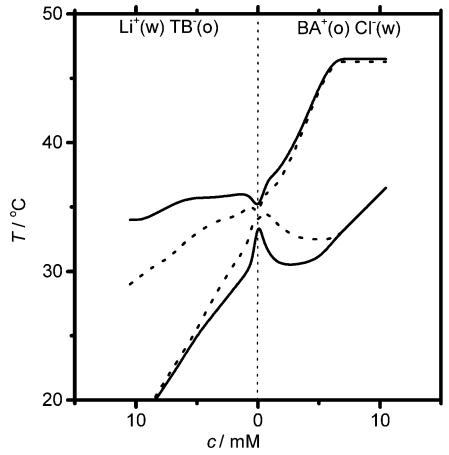

Figure 6. Dependence of the phase behavior of a 15% NP10, 42.5% H_2O, and 42.5% TFT microemulsion on the concentration of LiTB and BACl. The solid line represents the microemulsion failure lines and the dotted line the coexistence of the lamellar phase and bicontinuous phases.

It is widely accepted that when the temperature of the one phase microemulsion is increased, the oxyethylene−water interactions become weaker and phase separation occurs when the upper emulsification failure boundary is reached. This upper boundary of the one phase body may increase or decrease with the salt concentration. The increasing behavior is associated with the salting-in effect and reflects an increased solubility of the surfactant in water. Conversely, the decreasing behavior (salting-out) indicates a reduced solubility due to a dehydration of the surfactant EO moieties. The interpretations of these solubility changes are often based on the structure-breaking ability of the ions, with the anions having a larger influence than the cations. In particular, large, polarizable inorganic anions like iodide and thiocyanate have been found to destructure water and favor the solubility of the surfactant (salting-in).[35] Other ions like sodium and potassium are structure enhancers, which results in lower hydration and solubility of the surfactant (salting-out). An additivity law was proposed to identify the contributions of the individual ions forming the electrolyte. As a result, it was also found that the structure-forming lithium ion contributes to the salting-in effect, and the structure-breaking chloride ion contributes to the salting-out effect,[35] in accordance with its position in the

dx.doi.org/10.1021/la404263v | Langmuir 2013, 29, 15738−15746

Hofmeister series but in contradiction with the observation made above for other structure-breaking ions like iodide showing a strong salting-in effect. It has been concluded that the structure-breaking properties of the ions cannot solely explain the observed changes in the upper emulsification failure boundary.[36] The salting-out strength of inorganic salts in nonionic microemulsions has been shown to correlate with the Henry constant describing the electrolyte adsorption isotherms at the surfactant monolayer. Thus, for instance, the salting in effect of large polarizable anions like thiocyanate is not only related to its structure-breaking capacity but also with its stronger tendency to adsorb.[17] Moreover, since the microemulsions under study contain 10 mM LiOH (with respect to the aqueous phase), it is also relevant to mention that changing pH has been found to have a similar effect to adding electrolyte. In particular, increasing the pH in microemulsions with nonionic surfactants reduces the temperature of the upper emulsification failure boundary, that is, OH^- has a strong salting-out effect.[37]

The effects on inorganic salts on the phase diagrams of microemulsions with nonionic surfactants have been thoroughly studied theoretically and experimentally. A large effort has been devoted to explain the possible reasons (e.g., dispersion forces) regions with lower or higher salt concentration (as compared to the bulk) may form around the EO surfactant moieties and hence affect their interaction with water molecules.[36,38] Yet, a clear physical picture of what ions actually cause salting-in and salting-out effects has not been found.

The case of electrified microemulsions containing potential determining salts is, obviously, much more complex. Although the surfactant is nonionic, the preferential solvation of the ions makes them separate in different phases and accumulate at both sides of the surfactant monolayer, which also results in an electrostatic stabilization of the interface.[20] The effect of the partitioning salts on the PIT observed in this work is 2−3 orders of magnitude larger than what has typically been observed for the addition of common salts to microemulsions,[18] while addition of 10 mM LiOH or NaCl has negligible effect on the PIT, and thus the effect is likely to result from electrostatic effects rather than conventional salting-in/out due to structure breaking or making ions. The most obvious difference between BACl and LiTB is that the charges on the hydrophilic and hydrophobic ions are reversed and hence the direction of the interfacial electric field is also reversed. The field set by the partitioning salt can reach magnitudes of 100 mV/m, which is comparable to that used for orientation of liquid crystals, and may influence the curvature of the monolayer by orienting the surfactant molecules. However, when the field is reversed also the ion attracted to the interface changes, and consequently ion dependent penetration into the surfactant monolayer should be considered. On the water side, ion penetration into the palisade layer has been shown to follow the Hofmeister effect.[17] Different penetration of anions (OH^-, Cl^-) and cations (Na^+, Li^+) into the palisade layer would result in asymmetry of the double layer structures with respect to the point of zero charge, and consequently moments of the transverse pressure profile and curvature which depend on the sign of the polarization of the interface.[23] The thickness of the double layer extending into the solvents can be reduced by adding electrolyte that screens the interfacial charge in the respective phase. Addition of 10 mM LiOH or 10 mM NaCl had a negligible influence on the effect of LiTB and BACl, which indicates that the double layer extending into the aquenous phase is not important for the phenomenon.

SUMMARY

We have studied potential determining salts, composed of a hydrophobic and a hydrophilic ion in microemulsions. Due to the dominating interfacial area in the microemulsion, the salts can dissociate across the surfactant monolayer, thus creating oppositely charged oil and water domains. The charging results in back-to-back double layers in the oil and water phases, which increases the repulsion between the surfactant monolayers. This is reflected in the compressibility and bending elasticity of the surfactant monolayer, and consequently stabilization of the lamella in comparison to the bicontinuous phase. The salt also increases the stability of the microemulsion, by the energy gained from solvating the hydrophobic ion in oil and the hydrophilic in water, thus extending the temperature and surfactant ranges spanned by microemulsion body.

ASSOCIATED CONTENT

Supporting Information

Additional chain length distribution and MS data. This material is available free of charge via the Internet at http://pubs.acs.org.

AUTHOR INFORMATION

Corresponding Author

*E-mail: cjohans@cc.hut.fi.

Notes

The authors declare no competing financial interest.

ACKNOWLEDGMENTS

The academy of Finland is greatly acknowledged for financial support.

REFERENCES

(1) Danielsson, I.; Lindman, B. The definition of microemulsion. *Colloids Surf., A* **1981**, *3*, 391−392.

(2) Gavach, C.; Seta, P.; d'Epenoux, B. The double layer and ion adsorption at the interface between two non miscible solutions: Part I. Interfacial tension measurements for the water-nitrobenzene tetraalkylammonium bromide systems. *J. Electroanal. Chem.* **1977**, *83*, 225−235.

(3) Markin, V. S.; Volkov, A. G. Distribution potential in small liquid−liquid systems. *J. Phys. Chem.* **2004**, *108*, 13807−13812.

(4) Evilevitch, A.; Lobaskin, V.; Olsson, U.; Linse, P.; Schurtenberger, P. Structure and transport properties of a charged spherical microemulsion system. *Langmuir* **2001**, *17*, 1043−1053.

(5) de Gennes, P. G.; Taupin, C. Microemulsions and the flexibility of oil/water interfaces. *J. Phys. Chem.* **1982**, *86*, 2294−2304.

(6) Helfrich, W. Elastic properties of lipid bilayers. Theory and possible experiments. *Z. Naturforsch., C: Biochem., Biophys., Biol., Virol.* **1973**, *28C*, 693−703.

(7) Andelman, D.; Cates, P. G.; Roux, D.; Safran, S. A. Structure and phase equilibria of microemulsions. *J. Chem. Phys.* **1987**, *87*, 7229−7241.

(8) Daicic, J.; Olsson, O.; Wennerström, H. Phase equilibria of balanced microemulsions. *Langmuir* **1995**, *11*, 2451−2458.

(9) Golubovic, L.; Lubensky, T. C. Thermal fluctuations and phase equilibrium in microemulsions. *Phys. Rev. A* **1990**, *41*, 4343−4366.

(10) Gompper, G.; Schick, M. In *Phase Transitions and Critical Phenomena*; Domb, C., Lebowitz, J. L., Eds.; Academic Press: London, 1994.

(11) Widom, B. A model microemulsion. *J. Chem. Phys.* **1984**, *81*, 1030−1046.

(12) Strey, R. Microemulsion microstructure and interfacial curvature. *Colloid Polym. Sci.* **1994**, *272*, 1005−1019.
(13) Olsson, U.; Wennerström, H. Globular and bicontinuous phases of nonionic surfactant films. *Adv. Colloid Interface Sci.* **1994**, *49*, 113−146.
(14) Bryskhe, K.; Bulut, S.; Olsson, U. Vesicle formation from temperature jumps in a nonionic surfactant system. *J. Phys. Chem. B* **2005**, *109*, 9265−9274.
(15) Kahlweit, M.; Lessner, E.; Strey, R. Phase behavior of quaternary systems of the type water-oil-nonionic surfactant-inorganic electrolyte. 2. *J. Phys. Chem.* **1984**, *88*, 1937−1944.
(16) Kahlweit, M.; Strey, R.; Haase, D. Phase behavior of multicomponent systems water-oil-amphiphile-electrolyte. 3. *J. Phys. Chem.* **1985**, *89*, 163−171.
(17) Kabalnov, A.; Olsson, U.; Wennerström, H. Salt effects on nonionic microemulsions are driven by adsorption/depletion at the surfactant monolayer. *J. Phys. Chem.* **1995**, *99*, 6220−6230.
(18) Kahlweit, M.; Strey, R.; Firman, P.; Haase, D.; Jen, J.; Shomäcker, R. General patterns of the phase behavior of mixtures of water, nonpolar solvents, amphiphiles, and electrolytes. 1. *Langmuir* **1988**, *4*, 499−511.
(19) Kahlweit, M.; Strey, R.; Haase, D.; Firman, P. Properties of the three-phase bodies in water-oil-nonionic amphiphile mixtures. *Langmuir* **1988**, *4*, 785.
(20) Sottman, T.; Stubenrauch, C. Phase behaviour, interfacial tension and microstructure of microemulsions. In *Microemulsions: Background, New Concepts, Applications, Perspectives*; Stubenrauch, C., Ed.; John Wiley and Sons (Blackwell Publ.): Chichester, 2009; Chapter 1.
(21) Rajagopalan, V.; Bagger-Jörgensen, H.; Fukuda, K.; Olsson, U.; Jönsson, B. *Langmuir* **1996**, *12*, 2939−2946.
(22) Vierros, S.; Iivonen, T.; Johans, C. Measurement of the potential across the oil−water interface in microemulsion. *Electrochem. Commun.* **2012**, *20*, 33−35.
(23) Daicic, J.; Fogden, A.; Carlsson, I.; Wennerström, H.; Jönsson, B. Bending of ionic surfactant monolayers. *Phys. Rev. E* **1996**, *54*, 3984−3998.
(24) Katchalsky, A. Polyelectrolytes. *Pure Appl. Chem.* **1971**, *26*, 327−373.
(25) Olaya, A. J.; Ge, P.; Girault, H. H. Ion transfer across the water| trifluorotoluene interface. *Electrochem. Commun.* **2012**, *19*, 101−104.
(26) Olaya, A. J.; Méndez, M. A.; Cortes-Salazar, F.; Girault, H. H. Voltammetric determination of extreme standard Gibbs ion transfer energy. *J. Electroanal. Chem.* **2010**, *644*, 60−66.
(27) Free energies of transfer were calculated from the data given in refs 24 and 25 using a linear relationship between the transfer energies in water-1,2-dichlorotethane, and water-TFT. The data given in ref 24 was corrected to a viscosity of 0.5 mPa s.
(28) Lancaster, S. J.; Bochmann, M. Anionic ansa-zirconocenes with pentafluorophenyl-substituted borato bridges. *Organometallics* **2001**, *20*, 2093−2101.
(29) Campbell, R. F.; Melrovitch, E.; Freed, J. H. Slow-motional NMR line shapes for very anisotropic rotational diffusion. Phosphorus-31 NMR of phospholipids. *J. Phys. Chem.* **1979**, *83*, 525−533.
(30) Nallet, F.; Laversanne, R.; Roux, D. Modeling X-ray or neutron scattering spectra of lyotropic lamellar phases: interplay between form and structure factors. *J. Phys. II: France* **1993**, *3*, 487−502.
(31) Caillé, A. X-ray scattering in smectic A. *C. R. Seances Acad. Sci., Ser. B* **1972**, *274*, 891−893.
(32) Fogden, A.; Ninham, B. W. The bending modulus of ionic lamellar phases. *Langmuir* **1991**, *7*, 590.
(33) Evans, D. F.; Wennerström, H. *The Colloidal Domain*, 2nd ed.; Wiley: New York, 1999; p 230.
(34) Olsson, U.; Würz, U.; Strey, R. Cylinders and bilayers in a ternary nonionic surfactant system. *J. Phys. Chem.* **1993**, *97*, 4535−4539.
(35) Holtzscherer, C.; Candau, F. Salt effect on solutions of nonionic surfactants and its influence on the stability of polymerized microemulsions. *J. Colloid Interface Sci.* **1988**, *125*, 97−110.
(36) Weckström, K.; Zulauf, M. Lower consolute boundaries of a poly(oxyethylene) surfactant in aqueous solutions of monovalent salts. *J. Chem. Soc. Faraday Trans. 1* **1985**, *81*, 2947−2958.
(37) Magno, M.; Angelescu, D. G.; Stubenrauch, C. Phase diagrams of non-ionic microemulsions containing reacting agents and metal salts for the synthesis of bimetallic nanoparticles. *Colloids Surf., A: Physicochem. Eng. Aspects* **2009**, *348*, 116−123.
(38) Ninham, B. W.; Yaminsky, V. Ion binding and ion specificity: The Hofmeister effect and Onsager and Lifshitz theories. *Langmuir* **1997**, *13*, 2097−2108.

Supporting Information

Potential determining salts in microemulsions: interfacial distribution and effect on the phase behavior

Christoffer Johans[a,*], *Manja A. Behrens*[b], *Karl Erik Bergquist*[b], *Ulf Olsson*[b], *José A. Manzanares*[c]

[a]Department of chemistry, Aalto University, PO Box 16100, FI-00076 Aalto, Finland, [b]Physical Chemistry, Lund University, PO Box 124 SE-221 00 Lund, Sweden, [c]University of Valencia, Faculty of Physics, Department of Thermodynamics, c/Dr. Moliner, 50, E-46100 Burjasot, Spain

1. Introduction

Tergitol NP-10 is a surfactant with a hydrophobic nonyl phenyl group and a hydrophilic head group with an average of ten ethylene oxide units. Although the average number of ethylene oxide units are constant the distribution of chain lengths strongly affect the properties of the surfactant. The most important parameter that determines the characteristic is the cloud point, since it is very sensitive to the chain length distribution [A]. For Tergitol NP-10 the cloud point was 63 °C.

The chain length distribution surfactant was analysed using a liquid chromatograph (Waters, Acquity UPLC) coupled to a TOF- mass spectrometer (Micromass, LCT Premier) [B]. A 1:1 methanol:water eluent was used.

The mass spectrum of the sample is shown in Figure A. The peaks correspond to nonylphenyl based surfactant with variable head group lengths, charged by H^+ and Na^+ as assigned in the figure. $C_{15}H_{24}O(C_2H_4O)_{10}$ charged with one H+ was observed at 661.4 g/mol.

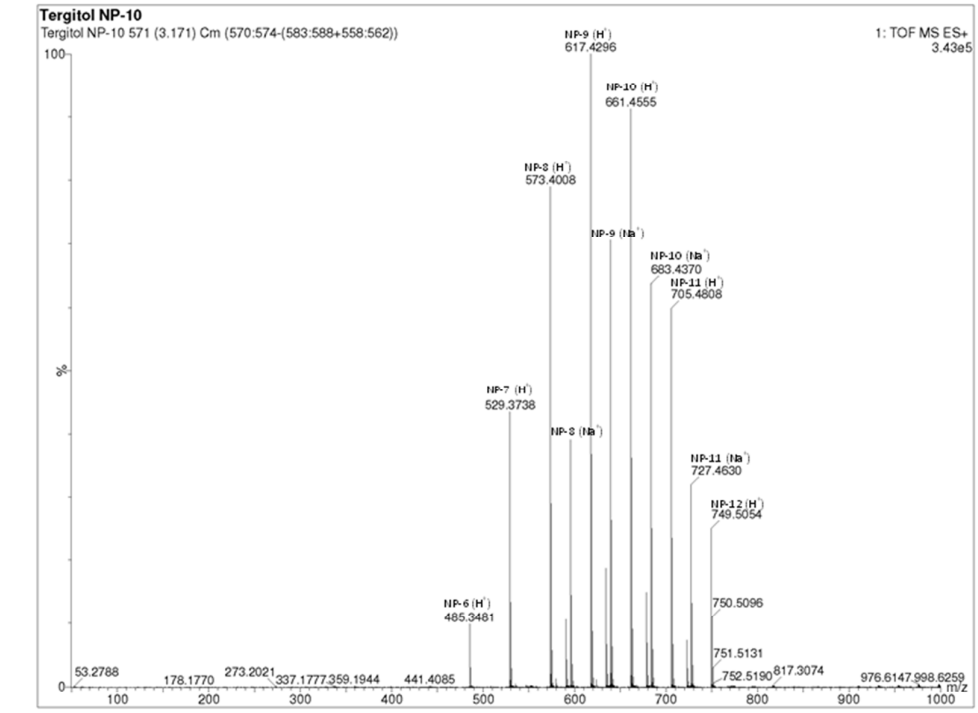

Figure A. The structure of a) the TB- ion, b) the BA+ ion and c) the Tergitol NP-10 surfactant.

The chain length distribution was calculated under the assumption that the peak height directly corresponds to the amount of the considered species in the sample and normalized with the most frequent component, which in this case was C15H24O(C2H4O)9. The average number of EO units per surfactant was 9.25, which is in slight contradiction with the reported value of 10.

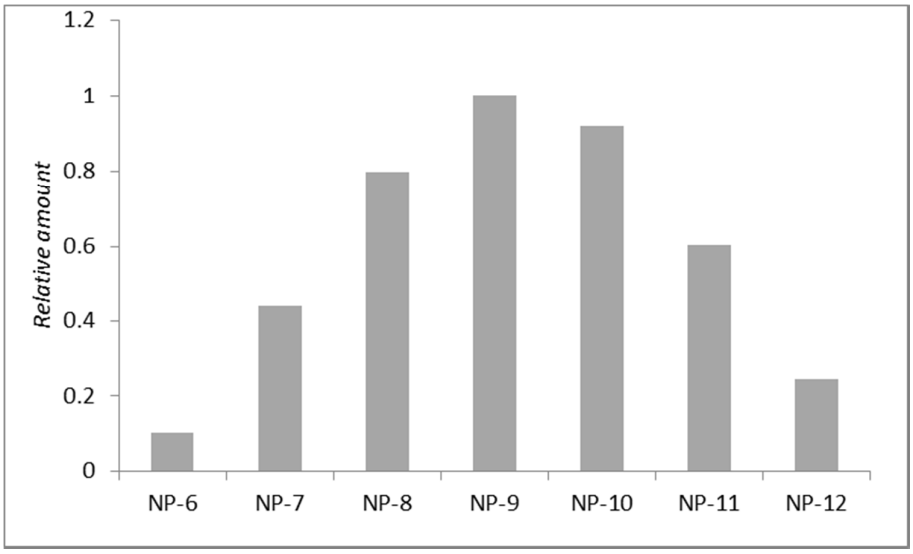

Figure B. Chain length distribution in Tergitol NP-10 calculated from the LC-MS spectrum.

[A] Toerne, K., Jackson, R., von Wandruszka, R. POE chain length selectivity in the clouding of a triton surfactant, *J. Coll. Int. Sci.* 2003, 257, 412-414.